



POLITECNICO
MILANO 1863

SCUOLA DI INGEGNERIA INDUSTRIALE
E DELL'INFORMAZIONE

EXECUTIVE SUMMARY OF THE THESIS

Functional and biomechanical evaluation of lumbar spinal stenosis patients during forward flexion and lateral bending using musculoskeletal modeling

LAUREA MAGISTRALE IN BIOMEDICAL ENGINEERING - INGEGNERIA BIOMEDICA

Author: GINEVRA ALAIMO

Advisor:

PROF. DR. LUIGI LA BARBERA

PROF. DR. STEPHEN FERGUSON

Co-advisor: ALICE CAIMI

Academic year: 2024-2025

1. Introduction

Lumbar spinal stenosis (LSS) is among the most common spinal disorders and represents one of the main reasons for spinal surgery in individuals over the age of 65 [1]. This condition is characterized by a narrowing of the neural canal and foramina, leading to the compression of the nerve roots or the cauda equina. This results in pain and functional limitations that significantly impair daily activities and overall quality of life. It is mostly acquired as a consequence of age-related degenerative changes affecting the lumbar intervertebral discs and facet joint, and can occur in three distinct anatomical sites, frequently in combination[1]. Central canal stenosis most often results from ligaments hypertrophy and intravertebral disc protrusion. Subarticular canal stenosis typically develops due to degenerative ligamentous and superior facet hypertrophy. Finally, intervertebral foramen stenosis arises from osteophyte formation beneath the pars interarticularis where the ligamentum flavum is attached or from hy-

pertrophy of bursal tissue in association with spondylitic defect.

Despite the available therapeutic options, that can be more conservative or invasive, many patients continue to experience functional limitations and characteristic symptoms associated with LSS. The most typical manifestation is neurogenic claudication [1], a discomfort radiating from the lumbar region to the buttocks and frequently to the thigh and lower leg, often associated with sensory loss, fatigue, weakness and balance problems. Symptoms are typically exacerbated by standing or walking, particularly during lumbar extension, which further narrows the spinal canal and, on the other hand, the symptoms are alleviated by sitting or forward bending, which increases canal dimensions [2]. Other compensatory strategies include reduced stride length and gait speed, asymmetric gait pattern, for ward flexed trunk posture and reduced lumbar lordosis, increased pelvic rigidity and greater knee flexion compared to healthy subjects. Although these compensatory mechanisms may temporarily alleviate symptoms, they

can alter spinal alignment and paraspinal muscle recruitment in order to maintain dynamic balance. Such alterations may lead to increased segmental spinal loads, thereby predisposing elderly patients, already affected by age-related muscle loss, to vertebral fractures and potentially increasing the risk of symptom recurrence and disease progression.

Despite the clinical relevance of this question, very few studies have quantitatively assessed spinal loads in patients with lumbar spinal stenosis, and existing analyses are mostly limited to walking tasks. Therefore, this project aims to fill the clinical and scientific gap with the evaluation of functional and biomechanical alterations in patients with lumbar spinal stenosis during forward flexion and lateral bending, which are functional movements representative of daily activities. To analyze patient-specific spinal alignment, kinematics, and internal loads during forward flexion and lateral bending, the study uses and applies an existing AnyBody motion capture driven musculoskeletal model [[3], [4]] integrated with radiographic alignment and motion capture data, to better characterize the functional and mechanical implications of LSS.

2. Methods

2.1. Patient Dataset

The study included 121 patients diagnosed with lumbar spinal stenosis who were recruited from the Department of Spine Surgery at the University Hospital of Basel and who underwent clinical assessment, performed standardized motor tasks, and completed several patient-reported outcome measures (PROMs) assessing overall health status, symptom severity, and kinesiophobia.

2.2. Kinematic Data Acquisition

To capture whole-body and spine kinematics, a total of 72 retroreflective markers were applied on the entire body of the participants and on the spinous processes from C7 to S1 levels. This extended configuration allowed a detailed representation of spinal curvature and segmental motion of body segments, enabling the determination of joint position and angles during the two motor tasks of forward flexion and lateral

bending. Marker data were pre-processed using the Vicon Nexus software, which included identification and labeling of trajectories, as well as gap filling through interpolation algorithms to handle short occlusions of markers (figure 1). After preprocessing, the data were exported in .c3d format, containing the three-dimensional trajectories of all optical markers, and imported into the AnyBody Modeling System (AnyBody Technology A/S, Aalborg, Denmark). Within this environment, the trajectories were used to drive the motion capture-based musculoskeletal model.

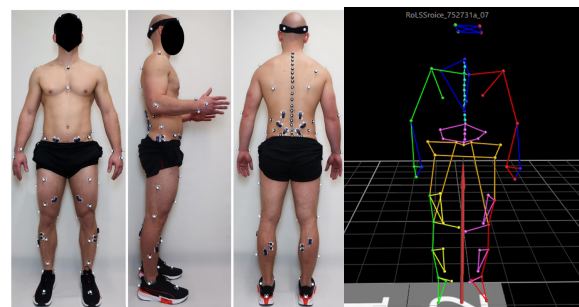


Figure 1: Placement of the retroreflective markers (left) and reconstruction of the trajectories in Vicon (right).

2.3. Spinal Alignment Assessment

To further enhance the patient-specific nature of the study, the posture of each participant was reconstructed using low-dose EOS radiographs acquired in standardized posture. Vertebral endplates were manually annotated in the KEOPS Balance Analyzer software, and the resulting pixel coordinates were imported into a MATLAB pipeline to compute vertebral centroids and orientations, as shown in figure 2. These spinal parameters were calculated from C2 to L5 and centroid coordinates from C2 to S1, and the exported into .any files, together with the lumbar lordosis (LL), thoracic kyphosis (TK), sacral slope (SS), and other subject-specific information such as body mass and weight. Each patient therefore had dedicated input file (in a .any format), which were used to scale the AnyBody musculoskeletal models.

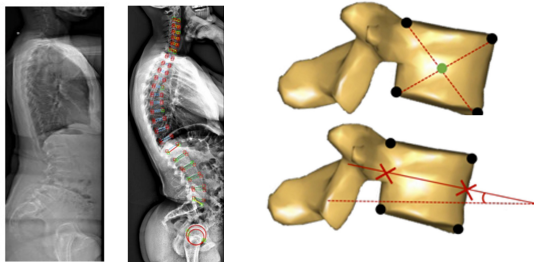


Figure 2: Manual vertebral annotation in KEOPS (left) and calculation of vertebral angles and centroids through a MATLAB pipeline (right).

2.4. Patient Specific Musculoskeletal Modeling

Patient-specific simulations were conducted using the AnyBody Modeling System (version 8.1 Beta), which combines a generic musculoskeletal model with a full-body motion capture framework and a detailed thoracolumbar spine module (figure 3). The model was enhanced through patient-specific ribcage scaling, determined by the ratio between the overall trunk length (T1–S1) and the thoracic length (T1–T12), and further refined by integrating sagittal spinal alignment parameters such as thoracic kyphosis and lumbar lordosis. In addition, the intervertebral disc behavior was improved by implementing level-specific stiffness equations for each vertebral segment, based on previous studies reported in the literature.

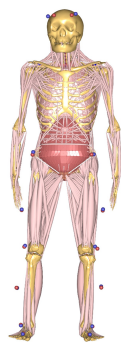


Figure 3: The complete full-body mocap musculoskeletal model.

Each model underwent an initial homogeneous anthropometric scaling based on the participant’s height and body mass. A subsequent marker-based optimization was then performed in AnyBody to minimize the distance between physical and virtual markers during an upright standing trial. This optimization adjusted bone segment lengths and virtual marker posi-

tions, ensuring accurate correspondence between recorded and simulated motion. The resulting configuration was saved for each subject in an .anyscript file, which contained the orientation and centroids of all vertebrae and the lengths of the corresponding bony segments. These individual parameter sets were then combined with the motion capture and radiographic data to produce fully patient-specific musculoskeletal models for biomechanical analysis.

2.5. Biomechanical and Statistical Analysis

Statistical analysis was carried out after verifying the normality of each variable using the Shapiro–Wilk test. Depending on the data distribution, Pearson or Spearman correlation coefficients were computed. To mitigate type I errors arising from multiple comparisons, all p-values were corrected using the Benjamini–Hochberg false discovery rate procedure. Comparisons with age-matched healthy subjects were performed using Welch’s t-test or Mann–Whitney tests, depending on the availability of raw data in the literature. Kinematic behaviour was analysed using a set of parameters that captured both spinal alignment and dynamic motion, including spinopelvic measures, trunk overall flexion, thoracic and lumbar range of motion (ROM), movement velocity, and segmental intervertebral motion. These variables were then associated to the spinal loads to identify which aspects of spinal motion contributed most to increased mechanical demand. Finally, the kinematic and kinetic measurements were associated with patient-reported outcome measures (PROMs), to understand the psychological impact of LSS. In addition, forward flexion was evaluated by comparing sagittal-plane motion and spinal loads of LSS population with those of an age-matched healthy cohort. For lateral bending, the analysis instead focused mainly on detecting asymmetries by comparing ipsilateral and contralateral bending, where ‘ipsilateral’ refers to bending on the same side as the stenosis and ‘contralateral’ to bending on the opposite side.

3. Results

3.1. Forward Flexion

Out of the 121 patients initially recruited, 101 were successfully simulated during the forward flexion task. The reduction in sample size was due to missing ground reaction force data, incomplete trials, or simulation errors, including muscle overloading or optimization failures.

During the forward flexion movement, patients with LSS exhibited a pronounced reduction in both global and segmental motion compared to a age matched healthy population [5]. The mean maximum trunk flexion angle reached $85.65^\circ \pm 15.62^\circ$, significantly lower than the $107.11^\circ \pm 17.41^\circ$ reported for healthy elderly controls. Both thoracic and lumbar contributions to total trunk flexion were reduced, with a mean thoracic range of motion of $10.3^\circ \pm 3.6^\circ$ and a lumbar range of motion of $28.3^\circ \pm 8.0^\circ$ in contrast with the healthy age matched population who typically exhibit $15.7^\circ \pm 7.3^\circ$ of thoracic and $46.4 \pm 11.0^\circ$ of lumbar mobility. The execution velocity of the task was found to be significantly higher in the healthy group than in the LSS group, respectively $12.66 \pm 9.94^\circ/\text{s}$ and $9.38 \pm 3.17^\circ/\text{s}$. At the segmental level, motion was consistently restricted across all lumbar segments and statistically reduced compared with age-matched healthy individuals. In patients with LSS, the mean flexion angles progressively decreased from $1.95^\circ \pm 0.61^\circ$ at L1–L2, $1.54^\circ \pm 0.56^\circ$ at L2–L3, $1.12^\circ \pm 0.49^\circ$ at L3–L4, $0.67^\circ \pm 0.43^\circ$ at L4–L5, and $0.21^\circ \pm 0.33^\circ$ at L5–S1, whereas healthy subjects exhibited substantially larger values of $7.00^\circ \pm 2.20^\circ$, $6.80^\circ \pm 2.00^\circ$, $7.00^\circ \pm 1.80^\circ$, $7.00^\circ \pm 1.70^\circ$, and $10.00^\circ \pm 3.10^\circ$, respectively. A significant correlation with stenosis severity was found at the L3–L4 level, one of the most frequently affected segments, where higher severity was associated with reduced segmental motion. Additionally, the flexion at the L3–L4 level was negatively correlated with the presence of spondylolisthesis, a condition that frequently coexists with lumbar spinal stenosis.

The analysis of spinal loads exhibited increased compression and shear forces throughout the lumbar region compared to the healthy age-matched population [5], as illustrated in figure 4, and were negatively correlated with the kinematic and spinal parameters.

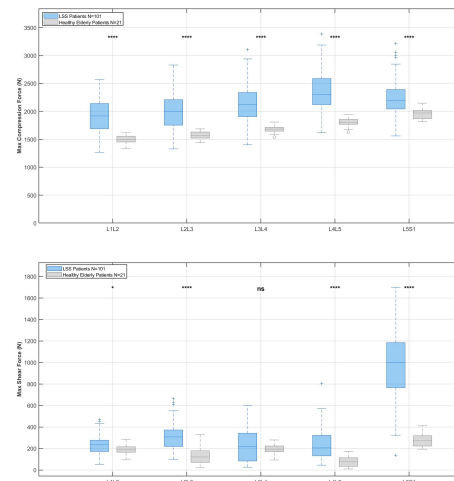


Figure 4: Maximum compressive forces (top) and maximum shear forces (bottom) estimated across the lumbar spine during the forward flexion task.

Higher scores on the PROMs, indicating higher pain, symptoms and kinesiophobia, were associated with reduced trunk and pelvic mobility, smaller maximum segmental flexion angles, and diminished thoracic and lumbar ranges of motion. Participants reporting higher disability demonstrated an increased thoracic kyphosis, reduced lumbar lordosis and increased pelvic rigidity.

3.2. Lateral Bending

For the lateral bending task, 98 patients were successfully simulated, where the reduction in the cohort is once again due to missing ground reaction force data, incomplete trials, or simulation errors, including muscle overloading or optimization failures.

The main research question was whether the presence of foraminal stenosis led to an asymmetric and different bending pattern between the affected and non-affected sides, and so the difference between right and left segmental bending was analyzed (figure 5).

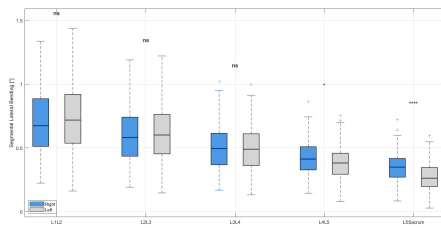


Figure 5: Comparison of the frontal segmental flexion on the right side (blue) and left side (left)

To further investigate the observed asymmetry in the L4–L5 and L5–Sacrum levels, lateral flexion to the right and left was analyzed separately in patients with right-sided and left-sided foraminal stenosis and revealed that the segmental bending in these the spinal level is greater to the right, independently to the position of the foraminal stenosis. To summarize, ipsilateral and contralateral flexion were compared, but no statistically significant differences were found between the two conditions.

Although, in patients with right-sided foraminal stenosis, the ratio between right and left trunk and lumbar range of motion progressively decreased with increasing stenosis grade (image 6, indicating a reduction in ipsilateral mobility or increase in the contralateral mobility).

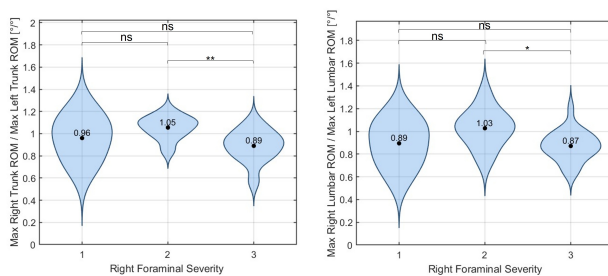


Figure 6: Violin plots showing the ratios between the maximum right and left trunk (left) and lumbar (right) range of motion across increasing grades of right foraminal stenosis severity.

Additionally, patients with a more severe right-sided foraminal stenosis tended to exhibit increased axial rotation during movement, rather than purely frontal-plane motion, as illustrated in figure 7.

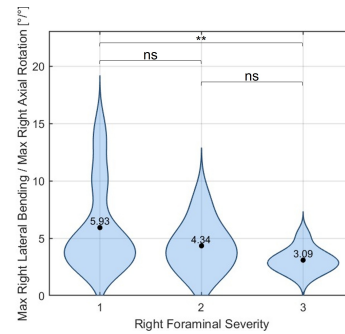


Figure 7: Violin plot comparing throughout severity levels the ratio between lateral bending and axial rotation.

Regarding spinal loads, lateral bending produced generally lower compression and shear forces than forward flexion, and correlated positively with the magnitude of bending angles, both globally and segmentally.

Patient-reported measures exhibited similar patterns of forward flexion. Higher scores of pain and presence of symptoms were associated with reduced trunk and segmental motion and with increased thoracic kyphosis, while elevated kinesiophobia corresponded to lower lumbar and thoracic range of motion.

4. Discussions

A major difference was observed between the two tasks: while trunk and segmental flexion correlated negatively with spinal loads during forward flexion, they showed a positive correlation during lateral bending. Infact, during during forward flexion, as the flexion increases, the contribution of passive spinal structures such as the intervertebral discs and ligaments becomes more relevant and support part of the applied load, thereby reducing muscular activity and compressive and shear forces. On the other hand, during lateral bending, the range of motion is more restricted and consequently the passive components are less engaged, and the muscular system remains the main contributor to spinal stabilization and load bearing.

During forward flexion, patients with LSS exhibited reduced global and segmental mobility compared with healthy controls, and the segmental flexion at the L3–L4 level, one of the most affected levels, is associated negatively with stenosis severity and spondylolisthesis, that could explain the more restricted motion.

Despite slower movement execution, patients showed significantly higher spinal loads, reflect-

ing altered biomechanics rather than dynamic effects. Such elevated loading may increase fracture risk in elderly individuals who may also suffer from other age-related degenerative conditions, such as osteoporosis or muscle weakness. The PROMs also reflected this restricted motion. Higher Oswestry Disability Index and Tampa Scale for Kinesiophobia scores were associated with smaller trunk and pelvic ranges of motion and reduced overall flexion. Moreover, patients reporting more severe symptoms tended to exhibit increased thoracic kyphosis, reduced lumbar lordosis, and greater pelvic rigidity, that are typical compensatory strategies adopted by individuals with LSS to alleviate neural compression. However, these compensatory patterns were not confirmed in the severity analysis, suggesting that they are more likely driven by psychological and behavioral factors rather than by structural impairment.

Regarding the lateral bending task, the main finding was a tendency toward greater segmental bending to the right, independent of the side of the foraminal stenosis, suggesting that the condition does not induce a clear asymmetry in movement. This may be explained by the fact that many patients presented bilateral foraminal stenosis, making it difficult to discriminate side-specific differences. In addition, part of the cohort exhibited a certain degree of scoliosis, which may have further influenced the movement pattern in the frontal plane. However, when focusing specifically on patients with right-sided foraminal stenosis, a different trend was observed. As the severity of the stenosis increased, both the ratio between right and left trunk ROM and the ratio between right and left lumbar ROM progressively decreased. These findings suggest that, despite the overall absence of a population-level asymmetry, patients with more severe right-sided stenosis tend to limit lateral bending toward the affected side, likely as a protective mechanism to avoid pain or neural compression during movement.

It was also observed that, with increasing severity of the right-sided foraminal stenosis, there was a decrease in the ratio between right lateral bending and right axial rotation, indicating that patients with more severe stenosis tend to add a greater component of axial rotation during bending.

5. Conclusions and future developments

LSS alters both movement patterns and mechanical load distribution during daily motor tasks. By examining biomechanics, structural alignment, and PROMs, this work provides a comprehensive framework for understanding the functional consequences of LSS and may guide future rehabilitation strategies.

The study presents several limitations. The musculoskeletal model relied on a simplified muscle representation rather than a Hill-type formulation, potentially leading to an overestimation of active muscle forces, relevant in particular during forward flexion where passive muscle components play a greater role in load support. Moreover, coronal alignment was not incorporated into the patient-specific reconstruction, limiting the ability to represent frontal-plane asymmetries that are especially relevant during the lateral bending task. The accuracy of marker-based kinematic reconstruction is also influenced by operator-dependent marker placement and soft tissue artefacts, particularly in individuals with higher BMI. Additionally, PROMs inherently reflect subjective perceptions of pain and disability, which may vary considerably across patients. Future developments should focus on integrating Hill-type muscle models and coronal alignment into the modeling pipeline, as well as incorporating subject-specific disc and paraspinal muscle degeneration to better capture the entire biomechanical effect of LSS.

6. Bibliography

References

- [1] Ciricillo SF and Weinstein PR. Lumbar spinal stenosis. *West J Med*, 1993.
- [2] Nowicki BH, Haughton VM, Schmidt TA, Lim TH, An HS, Riley LH 3rd, Yu L, and Hong JW. Occult lumbar lateral spinal stenosis in neural foramina subjected to physiologic loading. *American Journal of Neuroradiology*, 1996.
- [3] de Zee M, Hansen L, Wong C, Rasmussen J, , and Simonsen EB. A generic detailed

rigid-body lumbar spine model. *J Biomech*, 2007.

- [4] Ignasiak D., Dendorfer S., , and Fergusson S.J. Thoracolumbar spine model with articulated ribcage for the prediction of dynamic spinal loading. *J Biomech*, 2016.
- [5] Ignasiak D., Rüeger A., Sperr R., and Ferguson SJ. Thoracolumbar spine loading associated with kinematics of the young and the elderly during activities of daily living. *Journal of Biomechanics*, 2018.